The effects of screening length in the non-local screened-exchange functional

Yuzheng Guo[1], John Robertson[1] and Stewart J Clark[2]

[1]Engineering Department, Cambridge University, Cambridge CB2 1PZ, UK
[2]Physics Department, Durham University, Durham, DH1 3LE, UK

E-mail: s.j.clark@durham.ac.uk

Abstract. The screened exchange (sX) hybrid functional can give good band structures for simple *sp* bonded semiconductors and insulators, charge transfer insulators, Mott-Hubbard insulators, two dimensional systems and defect systems. This is particularly attributed to the sX hybrid scheme fixing the self-interaction problem associated with local functionals. We investigate the effect of varying the screening parameter of the exchange potential on various material properties such as the band gap. The Thomas Fermi screening scheme in which the screening parameter varies with an average valence electron density leads to a weak dependence of the band gap on valence electron density, so that a fixed screening parameter could be applied to heterogeneous systems like surfaces, interfaces and defects.

PACS numbers: 71.15.Mb, 71.15.Dx, 71.20.Mq, 71.20.Nr

1. Introduction

Density functional theory (DFT) has become the standard method to predict atomic and electronic properties in condensed matter physics and quantum chemistry[1, 2, 3]. The most widely used exchange-correlation functionals such as the local density approximation (LDA) or general gradient approximation (GGA) replace the exchange-correlation energy of the many-electron Schrödinger equation with a functional of the local electron density[4, 5]. DFT describes the ground state properties such as lattice constants and bulk modulus quite well at low computational cost. However, it is well known that both LDA and GGA underestimate the band gap in semiconductors and insulators as they do not give the energy discontinuity across the Fermi level as a function of electron occupancy[6, 7]. They also do not describe well localised states or strongly correlated systems such as Mott insulators[8] partly due to the absence of the self-interaction correction[9].

Various improvements have been suggested to overcome the drawbacks of LDA and GGA. One of the simplest is the DFT+U method[10, 11, 12]. This introduces a repulsive potential U on localised electrons as in the Hubbard model. This functional can be used for structural relaxation with low computational cost. However, this method strictly only applies to open shell systems such as the transition metal compounds, although it is now (often incorrectly) used as an empirical fitting method well outside its true range of physical validity[12]. Most semiconductors are close shell systems, for which DFT+U gives only limited improvements.

There are also more advanced methods such as the GW method based on the Greens function[13, 14, 15, 16, 17] and dynamical mean field theory (DMFT)[18]. In the GW approximation, the quasi-particle energy is calculated by expanding the electron self-energy and dielectric function. GW can give accurate band structures. However, it is computationally expensive, so that often only the first order perturbative version is used, referred to as G_0W_0. On the other hand, DMFT maps the many-body problem onto an impurity model without the approximation of independent electrons. It can cure some of the problems of DFT such as band gap under estimation and electron localisation, and has been widely used for actinides and Mott insulators. However, it is more costly than GW. This makes it computationally expensive to apply these methods to complex systems such as surfaces, interfaces, or defect supercells with hundreds of atoms. Thus, it is still desirable to find an accurate yet reasonably low cost DFT-style functional.

It is well known that the non-local Hartree-Fock (HF) potential tends to over-estimate band gaps while LDA tends to under-estimate band gaps[5, 6, 9]. Also, HF over-estimates localisation while LDA under-estimates localisation[9]. Hybrid functionals are a type of functional which empirically mixes a fraction of the HF potential with a local exchange-correlation functional and they can give reasonably correct band gaps and electron/hole localisations[19, 20]. Various hybrid functionals have been proposed such as B3LYP[20, 21], PBE0[22], and the Heyd-Scuseria-Ernzerhof (HSE)

functional[23, 24, 25]. These hybrid functionals are generalised Kohn-Sham functionals that can be used variationally for geometry optimisation just like LDA[20, 26]. These functionals are found to give good descriptions of the band gap in a variety of systems[28, 29, 30, 31].

Here, we discuss the screened exchange (sX) hybrid functional of Bylander and Kleinman[32]. This replaces the short range part of the LDA by a short-range screened Hartree-Fock exchange energy[26, 32, 33, 34, 35, 36, 37]. sX has been implemented for a plane wave basis within the CASTEP code[34]. Geometry optimisation was helped by a fast algorithm to calculate the Hellman-Feynman stress[38]. sX has been widely used in many band structure and defect calculations[33, 34, 35, 36, 37, 39, 40, 41, 42, 43]. The band gaps from sX of semiconductors are improved with a mean relative error of 7.4%[34].

The early papers on hybrid functionals used a fixed mixing parameter of α=0.25 (meaning 25% HF exchange) based on Becke's rationalisation[20]. HSE kept this value of α and varied the screening parameter between the HSE03 and HSE06 versions[24, 25]. On the other hand, some recent papers have varied the mixing fraction, noting that this parameter might vary with the band gap or the dielectric constant[44, 45] and that HSE under-estimates the band gap of very wide gap insulators[30]. On the other hand, Moussa *et al*[46] considered the optimisation of both parameters for some solids. The hybrid functionals have been analysed[47, 48, 49] and criticised[50] with respect to GW.

In the case of sX, the mixing fraction is kept at 1, and the screening parameter is chosen in terms of the screening arising from the valence electron density[34]. Nevertheless, it is interesting to see how the structural properties and band gap would vary if the screening parameter is allowed to vary. At one level, we find that the calculated band gap is rather insensitive to the valence electron density in this approximation. At another level, HSE chose a fixed screening parameter independent of system[24], a useful simplification when treating heterogeneous systems such as surfaces or interfaces between systems of electron density. Different approximations have been proposed to calculate the screening effects[50] but we find that the band gap is rather insensitive to screening parameter.

This paper is organised as follows. In the next section, we present the methods used in this work with special attention paid to the screening parameter. In section 3, we give detailed description of the effect of screening parameter on total energy, lattice constant, band structure, and defect calculation. In section 4, we discuss the results and finally draw conclusions from the results obtained in this work.

2. Methods

The sX functional is a non-local Schrödinger equation in which the exchange-correlation energy depends on both the electron density and electron orbitals,

$$\left[-\frac{1}{2}\nabla^2 + V_H[n(r)] + E_{\text{ext}}[n(r)] + V_{\text{loc}}^{\text{XC}}[n(r)]\right]\psi_i(r) +$$

$$\int V_{\mathrm{nl}}^{\mathrm{XC}}(r,r')\psi_i(r')dr' = \epsilon_i\psi_i(r) \tag{1}$$

where the term in brackets is the kinetic energy, the Hartree energy, the external potential, and the local XC energy such as the LDA or GGA part. The second part is the non-local part of XC energy which depends explicitly on electron orbitals. sX assumes that the HF exchange is screened by a Thomas-Fermi (TF) screening parameter, so the potential decays exponentially with the distance,

$$E_{nl}^{XC} = -\frac{1}{2}\sum_{ij,kq}\int\int drdr' \frac{\phi_{ik}^*(r)\phi_{ik}(r')\phi_{jq}^*(r')\phi_{jq}(r)}{|r-r'|}\exp\left(-k_{TF}\,|r-r'|\right) \tag{2}$$

where i and j label the electron bands, k and q for k-points, and k_{TF} is the TF screening parameter. The local part is modified to avoid the double counting of the local part of the screening potential,

$$E_{loc}^{XC} = E_{HEG}^{XC}\left[\rho(r)\right] - E_{NL-HEG}^{XC}\left[\rho(r)\right] \tag{3}$$

where the first term on the right is just the LDA functional. The second term is the non-local exchange-correlation energy of a homogeneous electron gas (HEG) with a density $\rho(r)$. Combining the local and non-local part gives the full exchange-correlation energy

$$E^{XC} = E_{nl}^{XC} + E_{loc}^{XC}. \tag{4}$$

The TF screening constant represents the screening range of the electron interaction. If $k_{TF} = 0$, the non-local XC becomes the full HF potential and the local part becomes the LDA correlation energy. Thus the result from HF limit should not be interpreted as comparable to the pure HF method or advanced methods such as exact exchange method (EXX). If k_{TF} is infinite, there is full screening. The HF part is screened away and the local part returns to LDA. Therefore sX gives the correct asymptotic limit of the free electron gas.

Figure 1 compares the screening in the different hybrid functionals. Figure 1(a) shows the screened fraction of the HF potential as a function of inter-electron distance. The HF fraction is a constant for PBE0. For the sX, the screening parameter is varied to show how this affects the HF fraction. As the increases the fraction of HF decreases and vice versa. The medium range, from 2 to 4Å, is an important range for this parameter because most inter-atomic distances fall into this range. Figure 1(b) compares the screening in reciprocal space. The HSE screening and sX screening with various screening parameters are compared with the dielectric function of GaAs[51]. We see that a TF screening parameter of 1-2Å^{-1} is close to that of the dielectric function.

In principle, we can achieve a good description of the electronic structure if the screening parameter is allowed to vary. Ideally, the screening parameter should be fixed by some procedure. If the TF screening model[52, 53] is used, the screening parameter is given by

$$k_{TF} = 2\sqrt{\frac{k_F}{\pi}} \tag{5}$$

Figure 1. (a) Comparison of HF potential fraction in different hybrid schemes. Different TF screening parameters are used in sX (green lines). For PBE0 (blue line) $\alpha = 0.25$. For HSE (red line), $\alpha = 0.25$ and $\mu = 0.2$. (b) Comparison of the inverse dielectric constant for different functionals. The same parameters as (a) have been used. The inverse dielectric function of GaAs has been plotted (black line) for comparison[51]. Note the similarity of sX screening to that of the experimental inverse dielectric function.

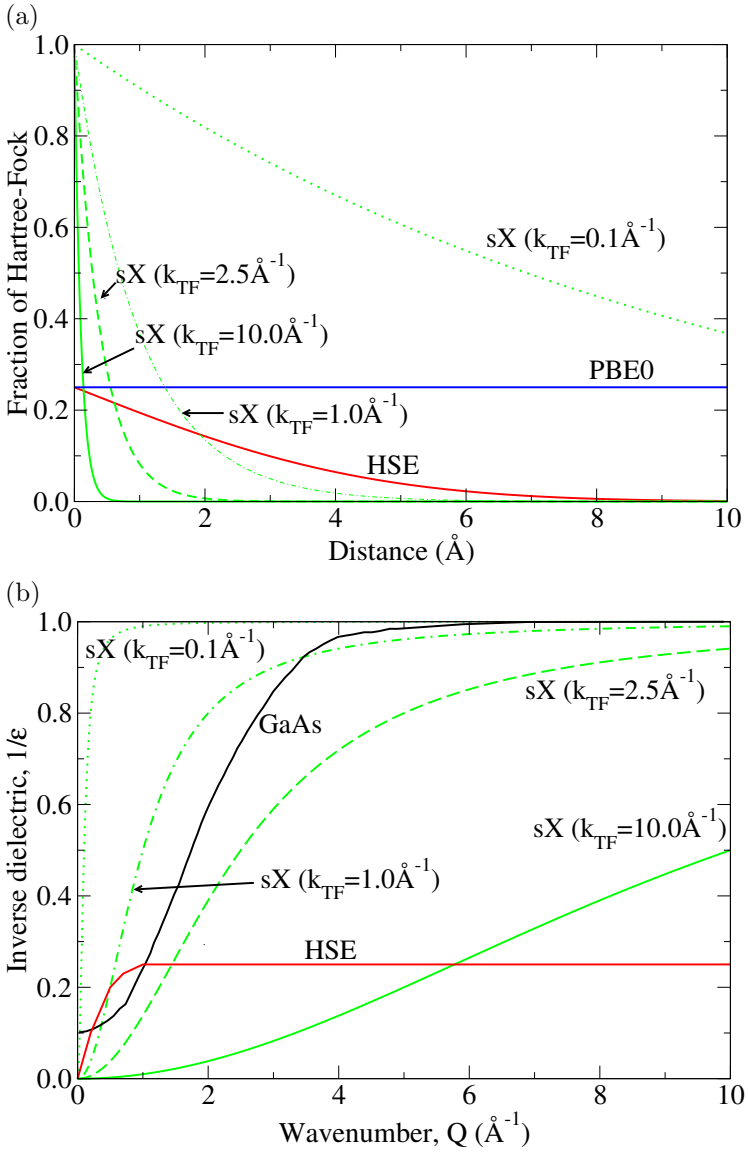

where k_F is the electron Fermi wavevector. We can also write k_{TF} in terms of electron density $\rho(r)$,

$$k_{TF} = 2\left(\frac{3\rho}{\pi}\right)^{\frac{1}{6}} \tag{6}$$

so the screening parameter is proportional to the one sixth order of valence electron density, which explains why the k_{TF} is a slowly varying function of $\rho(r)$. Unless stated otherwise, all the values used in this work is summarised in Table 1.

Table 1. The screening parameter used for different materials in units of $Å^{-1}$.

Material	k_{TF}
C	2.50
Si	2.09
Ge	2.06
GaAs	2.04
Al_2O_3	2.48
HfO_2	2.54
Ti_2O_3	2.43
Cr_2O_3	2.52
Fe_2O_3	2.56
BN	2.56

The plane wave basis pseudopotential package CASTEP is used to carry out all the calculations in this work[54]. The norm-conserving pseudo potentials are defined in Ref. 21, where most of them are the default pseudopotentials while some more transferable potentials are generated using the OPIUM code. A Monkhorst-Pack (MP) k-point mesh is used for the integration over the Brillouin zone[55]. The convergence of the total energy differences with respect to the mesh size and cutoff is better than 0.01 eV/atom. The density mixing scheme is used for electronic energy minimisation for most *sp* semiconductors, while a preconditioned conjugate-gradient scheme is used for most transition metals because the density mixing method can be unstable due to the orbital dependence of the functional[26].

3. Results

3.1. Wave function

It has been pointed out by several groups that the sX wave function can be almost identical to that from LDA/GGA in many cases[26]. We have confirmed this similarity. First of all the LDA/PBE wave function can be a good starting point for sX calculation. This greatly reduces the computational time. Furthermore the LDA/GGA wave function can be used for a sX band structure calculation:

$$\epsilon^{sX}_{n,k} = \left\langle \psi^{sX}_{n,k} \left| V^{sX}\left[\left\{\psi^{LDA}_{n',k'}\right\}\right] \right| \psi^{sX}_{n,k} \right\rangle . \tag{7}$$

The band structure from an LDA/PBE basis with an sX potential shares the similar curve as the self-consistent sX band structure. But the band gap is lower compared to a self-consistent sX calculation. Figure 2 compares the Si band gap as a function of the screening parameter from LDA/GGA with the self-consistent sX band gaps. The same $6 \times 6 \times 6$ MP grid has been used for reciprocal space integrations. The experimental crystal structure has been used for all cases. The difference between the sX and the LDA/GGA bands increases as the screening parameter decreases. At the HF limit, the error could be as be large as 25% of the band gap. However, the error is about 2%-3%

Figure 2. The calculated band gap of Si as function of screening parameter with difference wave functions from LDA (orange line), PBE (black line), and sX (green line). The figures shows that LDA and PBE wave function gives similar results when screening parameter is larger than 1. The difference becomes significant when approaching HF limit. The dashed line shows the experimental band gap.

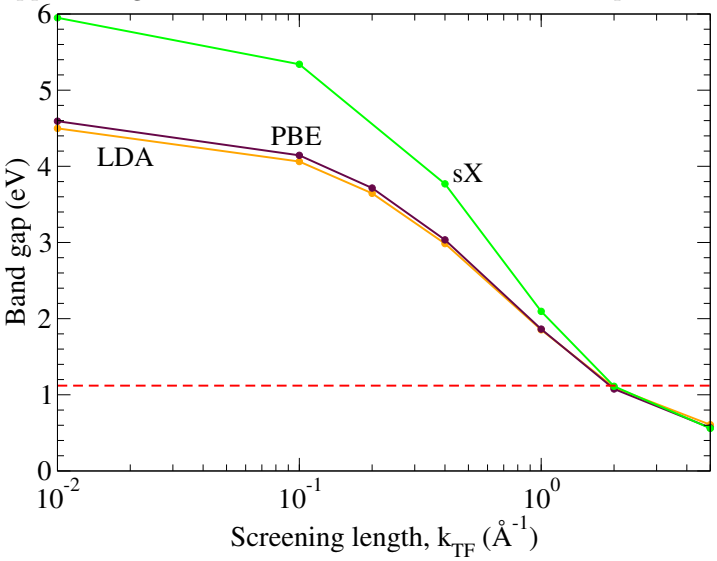

Table 2. sX band gaps (in eV) based on different wave functions.

Material	sX wavefunction	LDA wavefunction	Difference
C	5.32	5.04	0.28
Si	1.09	1.07	0.02
Ge	0.69	0.60	0.09
GaAs	1.52	1.47	0.05
Ti_2O_3	0.22	0.00	0.22
Cr_2O_3	3.56	3.48	0.08

for reasonable screening parameters of 1.8-2.5$Å^{-1}$, which suggests that the LDA/GGA wave function could be almost identical to the sX wave function, in agreement with previous results.

Table 2 shows the band gap of several solids with their respect the TF screening parameter using the LDA wave function or the sX wave function. The error induced by the LDA wave function is usually less than 0.2eV. Therefore, it is acceptable for most semiconductors and insulators. However, the LDA wave function should not be used for small band gap or correlated semiconductors. Ti_2O_3, a paramagnetic semiconductor, whose band gap is only 0.1-0.2eV, can be well described by the self-consistent sX with a band gap 0.22eV, but a LDA/GGA wave function will give a metallic band structure.

Figure 3. Variation of lattice parameter of Si with screening length (black line). The dashed line marks the experimental lattice parameter of 5.41Å. We see the usual LDA (large k_{TF}) overbinding and HF (small k_{TF}) overbinds further.

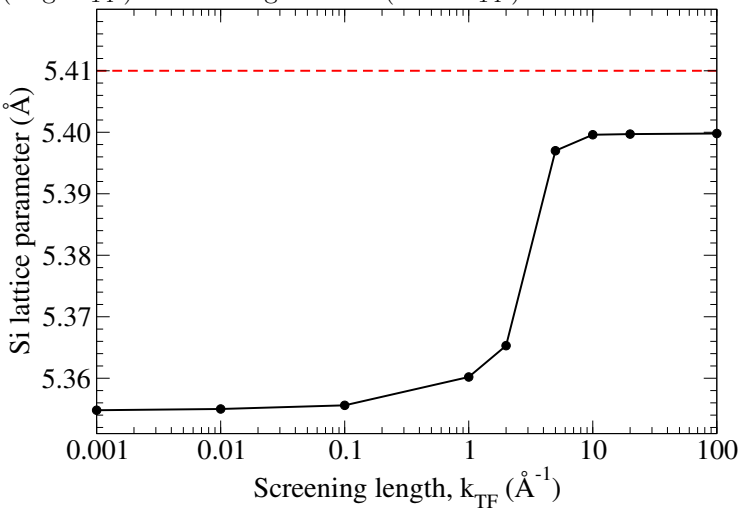

3.2. Lattice constant

We used sX to relax the lattice constant of Si to see the influence of various screening lengths, k_{TF}. The LDA is known to under-estimate lattice constants while GGA tends to over-estimate it (5.40Å and 5.46Å respectively). The sX hybrid functional mixes the screened HF potential and LDA local potential. The results are shown in Figure 3. The LDA gives 5.40Å which is below the experimental value, while the HF limit gives 5.355Å. This underestimate of lattice parameter using HF is expected given standard molecular results[27].

3.3. Band structure

The most important application of the sX hybrid functional is to correct the band gap problem in DFT. Here, the band structures are calculated with various screening parameters for various materials ranging from the simple *sp* semiconductors, to transition metal oxides with *d* electrons, Mott-Hubbard systems and 2-dimensional systems. The data is summarised in Figure 4. The gaps are normalised to the experimental band gap as 1 and to the band gap in the HF limit as 2, for each material. The experimental value of band gap gathers round a screening length of 1.8-2.5Å^{-1} which confirms that TF screening scheme gives a correct band gap. It has been shown previously that the sX functional can give much better band gaps in many *sp* semiconductors[32, 33, 34, 35, 36, 37, 38, 39, 40, 41, 42, 43]. Here we show the band gap variance as a function of the screening parameter. In order to eliminate the effect of lattice constants, we use the experimental lattice constants. Figure 4 shows the results from Si, C (diamond), Ge, and GaAs. The electron configuration and crystal structure are the same for these semiconductors, thus their TF screening parameters are similar. We see that the slope of the variation of band gap with screening parameter is smaller

Figure 4. The band gaps versus screening parameter for Si, C (diamond), Ge, GaAs, Al_2O_3, HfO_2, BN, Ti_2O_3, Cr_2O_3, Fe_2O_3, and Si(111)-(2 × 1) surface. The data is normalised by two limits, the experimental band gap and HF limit band gap (respectively, 1.0 and 2.0 on the vertical axis).

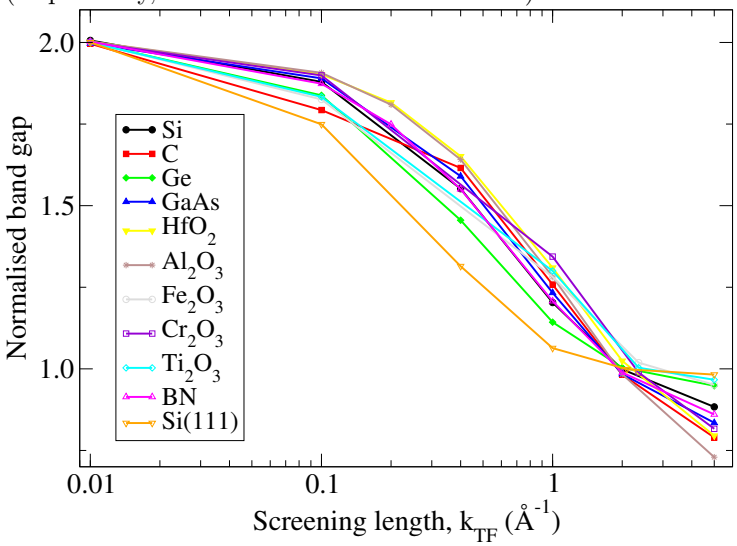

than the experimental band gap, so that the band gap is not so sensitive to the screening parameter. The error induced by a small deviation from the optimum TF value is quite small.

Figure 4 also shows the band gaps for the wide gap, closed-shell, insulators BN, HfO_2 and Al_2O_3. These insulators are important from both the scientific and technological points of view. HfO_2 and Al_2O_3 are the widely used as gate insulators in field effect transistors. Hexagonal BN is now used as a substrate for 2D systems such as graphene and MoS_2. We see that the normalised trend of band gap versus screening parameter is similar in all these systems, and that the optimum value is close to the TF value.

Another problem for the LDA/GGA functional is over delocalisation of semi-core states such as the d and f electrons. For the sp semiconductors only the band gap is under-estimated but the band structure is qualitatively correct. However LDA/GGA fails qualitatively for localised, open-shell, d and f electron systems. The LDA band gap disappears in systems such as the Mott-Hubbard insulators Ti_2O_3. We previously found that sX gives good band gaps for several transition metal oxides[41, 42] and that hybrid functionals in general can treat the transition metal and lanthanides well[31, 43].

Here, we have calculated the band gap of Ti_2O_3, Cr_2O_3, and Fe_2O_3 as a function of screening parameter as also shown in Figure 4. These transition metal oxides range from small band gap semiconductor to wide band gap semiconductor with both paramagnetic and anti-ferromagnetic ordering. sX was found to successfully describe all these systems. The experimental lattice constants are used for the primitive cells. Ti_2O_3 is a paramagnetic semiconductor with band gap of about 0.1eV. We noted above that sX with an LDA wavefunction will give a metallic band structure. The band gap does not

open up until the screening parameter is less than 5Å^{-1}. Cr_2O_3 is an anti-ferromagnetic insulator, intermediate between a charge transfer and Mott-Hubbard insulator. Fe_2O_3 is an anti-ferromagnetic Mott-Hubbard insulator. We see here that TF screening can also give a correct band gap for these correlated d electron systems.

Surface band structures might be quite different from the bulk band structures. Quantum confinement effects are quite important in quasi-2D surface band structures. It has been claimed that the hybrid functionals could not give the correct prediction of 2D and 1D systems[50]. However we find here that the sX functional with a similar TF screening can give a reasonable band gap of low-dimension systems. We previously found that sX will reproduce the Fermi velocity of graphene[40], which is under-estimated by LDA. Here we calculate the Si(111)-(2×1) surface as an example of a 2D system.

The Si(111)-(2×1) surface is a good test of a 2D system because of its well known atomic and electronic structure[56, 57, 58, 59, 60, 61]. Figure 5(a) shows that the (2×1) reconstruction causes the surface dangling bonds to form a π-bonded chain along the [011] direction.

In our calculation, the same pseudopotential and screening parameter from the bulk Si is used for the surface calculation and the bulk band structures. The surface is constructed from a 16-layer Si slab with 20Å of vacuum. Hydrogen is used to passivate the opposite side of the slab. The Brillouin zone is sampled with a $2\times4\times1$ k-point mesh. This supercell is found to converge the energy to within 0.01 eV with respect to the slab thickness. In order to eliminate the effects of geometry relaxation, the sX-relaxed structure with the bulk TF screening parameter is used during all calculations. The force is relaxed to less than 0.02eV/Å. The surface atomic structure from sX is almost the same as the PBE-relaxed structure as long as the same bulk lattice constant is used.

Figure 5(b) shows the surface band structure calculated in sX, compared to the surface states found by photoemission and inverse-photoemission[57], and also to the GW calculations of Northrup *et al*[61]. The band gap of the surface π-bonded chain is direct and at J. Most bulk semiconductors and insulators that we have discussed so far have small exciton binding energies, so that it is not necessary to distinguish between the optical gap and quasi-particle gaps. However, the exciton binding energy of the Si(111) surface is 0.28eV, much larger than the bulk binding energy of 0.015 eV[58]. Thus, the quasi-particle gap is significantly different from the optical gap. The calculated sX surface band gap is 0.45 eV. Interestingly, this is closer to the experimental optical band gap of 0.47 eV, but is 0.2 eV less than the experimental photoemission gap of 0.65 eV. This behaviour is unusual, but it is consistent with the observation of Scuseria *et al*[62] that the HSE band gap might be identified more with the optical gap.

Figure 6 shows the band gaps of Si(111)-(2×1) as a function of sX screening parameter. The figure shows similar trends as other systems. The error by TF screening with average electron density is less than 0.05eV. The slope of band gap versus screening parameter is relatively small around the experimental gap.

In order to compare the screening effects in 2D and 3D systems, we also consider the electronic structure and screening in bulk (3D) and monolayer (2D) MoS_2[63, 64, 65, 66].

Figure 5. (a) Geometric structure of Si(111)-(2 × 1) surface. (b) Band structure of the Si(111)-(2 × 1) surface from sX (black lines), comparing to band energies from photoemission (PE) and inverse photoemission (IPE) (triangle)[57], and GW quasi-particle energies (cross) from Northrup *et al*[61].

(a)

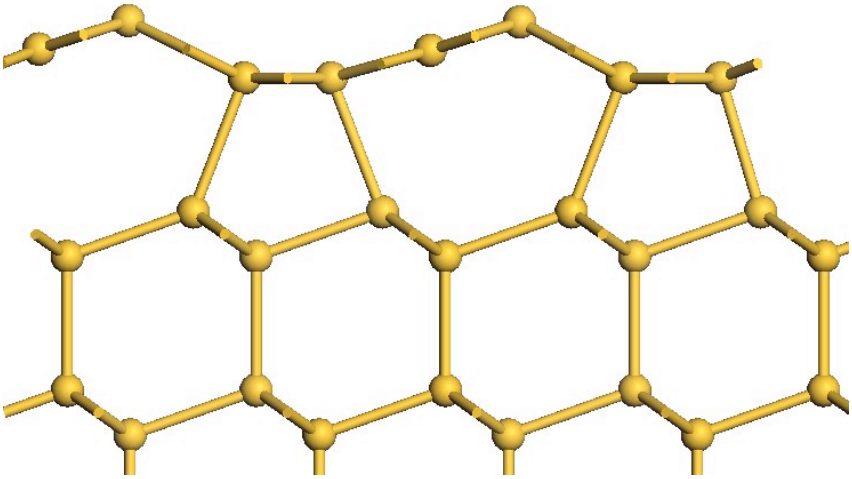

(b)

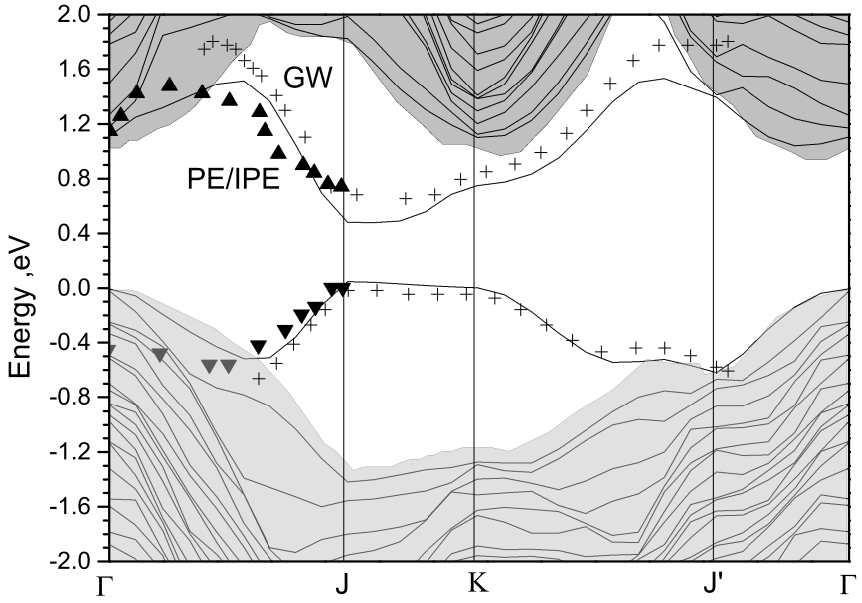

Figure 6. Variation of the calculated surface band gap of Si(111)-(2 × 1) with sX screening length.

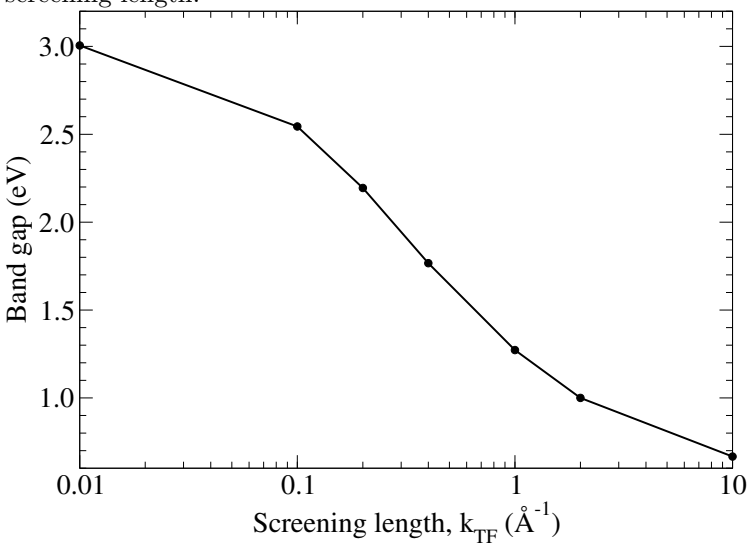

Here, the exciton binding energy is small in bulk MoS_2, whose band gap is 1.27 eV and indirect. In contrast, the exciton energy is large, of order 0.9 eV, in monolayer MoS_2[63, 64]. The minimum optical gap of monolayer MoS_2 is 1.88 eV and direct. The quasi-particle gap of monolayer and bulk MoS_2 is taken to be 2.7 eV from refs [63, 64]. This is consistent again with comment of Scuseria *et al* [62] that the HSE band gap might be identified more with the optical gap, not the quasi particle gap.

Our sX calculations of MoS_2 use the same pseudopotential and calculation parameters as in our previous work[66]. Figure 7(a) shows that the variation of band gap with screening parameter for 3D and 2D MoS_2. We see that the variation is the same when normalised to the optical gap (Figure7(b)). However, it is different if it is normalised to the quasi-particle gap, where the effect of low screening particularly affects the 2D system. These results illustrate that low dimensional systems are quite useful to study the effects of low screening, without going to wide gap systems.

To summarise, the TF average density method gives quite good band structures for all the systems studied so far. The band gap varies slowly for screening parameters around the TF value, 1.8-2.5$Å^{-1}$. This should allow us to use an average screening parameter for mixed systems such as interfaces or surfaces.

3.4. Charge transition level

The defect levels of semiconductors are an important application of hybrid functionals. The charge transition level is defined as the energy where the two charge states of the defect have the same formation energy. First-principles calculations are a useful tool to determine defect properties. However, semi-local XC functional are unlikely to get transition levels correct, due to the band gap problem. Moreover, the electron delocalisation problem of semi-local DFT can lead to the incorrect ground state for some

Figure 7. Dependence with respect to screening length of (a) minimum band gaps of 2D (curved dashed line) and 3D (curved solid line) MoS_2, and (b) normalised to the experimental optical gap. Experimental gaps are shown in (a) by the horizontal lines for 2D (dashed line, 1.88 eV) and 3D (solid line, 1.27 eV) materials and the quasiparticle gap also indicated (dot-dash line, 2.7 eV). Note in (b) the similar dependence of 2D and 3D when normalised to the optical gap (1.0 on the vertical axis). Both diagrams indicate that the same screening is suitable for both 2D and 3D materials.

(a)

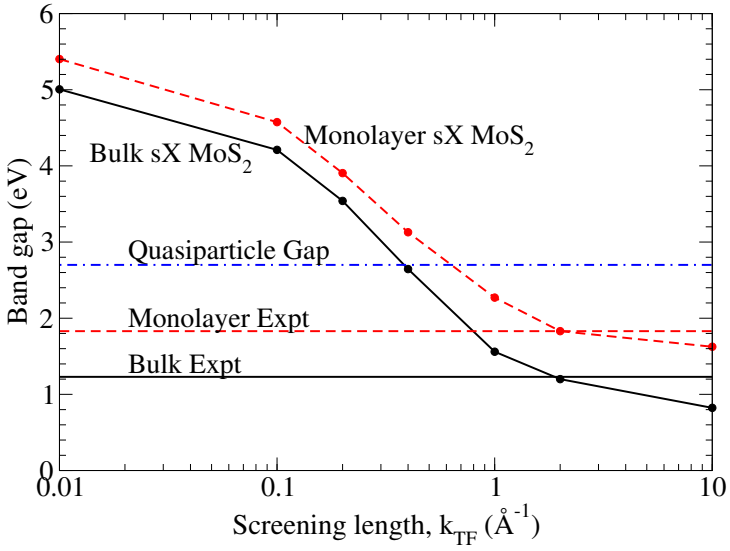

(b)

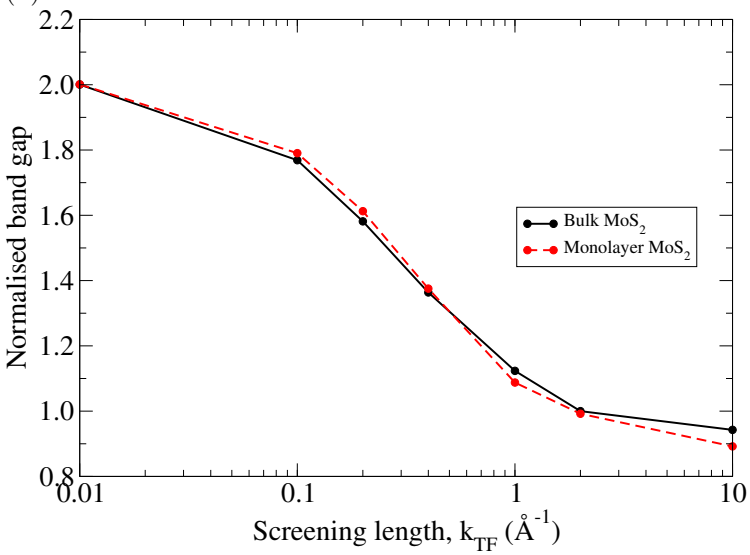

defects[67, 68, 69, 70]. The sX hybrid functional is known to correct these problems in several semiconductors and insulators[35, 39, 66, 71, 72]. HSE has been widely used in defect calculations. Here we investigate the effects of the sX screening parameter on the charge transition levels for the As anti-site centre in GaAs.

There are not so many cases where the defect is fully identified experimentally and the transition level is known. The As anti-site or EL2 centre in GaAs has been selected for this study. It is responsible for the Fermi level pinning in the mid band gap. It has been confirmed to give two transition states at 0.5eV (+ + /+) and 0.7eV (+/0) by experiments such as scanning tunneling spectroscopy, and electron paramagnetic resonance[72, 73]. Its atomic structure is also known from both experiments and DFT calculations[72, 73, 74, 75]. It is a rare case where both the atomic and electronic structure of the defect are known from experiments.

We used a 64-atom cubic super cell with one As anti-site. A $2 \times 2 \times 2$ MP grid is used for Brillouin zone integrations. The geometry is relaxed with the sX hybrid functional for each different screening parameter. The formation enthalpy is calculated for the 0, +, and ++ states. The total energy of the defect cell and the perfect cell are calculated for each charge state. The defect formation energy is then calculated as,

$$H_q\left(E_F,\mu\right) \,=\, \left[E_q - E_H\right] + q\left(E_V + \Delta E_F\right) + \sum_\alpha n_\alpha \left(\mu_\alpha^0 + \Delta\mu_\alpha\right) \qquad (8)$$

where E_q is the defect cell energy, E_H is the perfect cell energy, qE_V is the change in energy of the Fermi level when charge q is added and n_α is the number of atoms of species α. The charge correction process follows the procedure of our previous calculations[39].

Figure 8(a) plots the two defect transition levels as a function of the screening parameter. The difference between these two states remains constant at 0.1eV. As the HF part becomes larger, the transition level rises, just like the band gap. The sX hybrid functional gives a slightly higher transition level compared to experiment. However other hybrid functionals, such as HSE, also give higher transition levels for EL2[74, 75]. The error could be due to the small size of supercell and pseudopotentials without d electrons. However we note that the charge transition level is not shifted significantly for screening parameters of 1.8-2.3Å^{-1}. Figure 8(b) plots the transition energies as a fraction of the calculated band gap.

4. Discussion

We find that the sX hybrid functional works well for such a wide range of materials. Its success is based on the following two facts. First the screened exchange term can give the correct band structure for these materials due to the introduction of the long-range screened HF terms. Compared to LDA+U or LDA+DMFT where the weak correlation is still based on LDA, the sX hybrid functional could give a better description for the simple *sp* semiconductor and the strong correlated systems such as transition metal oxides at the same time. Secondly, the TF screening parameter which determines the fraction of HF exchange has only a weak effect on the band gap, around its optimum

Figure 8. (a) Calculated sX band gap (solid line) and the 0/+ (dashed line) and +/++ (dotted line) transition levels of the As anti-site in GaAs as a function of the sX screening parameter, in eV. (b) Transition levels (labels as in (a)) normalised to the GaAs band gap, as a function of screening length, k_{TF}. Note the levels fall as a fraction of the total band gap towards to HF limit on the left.

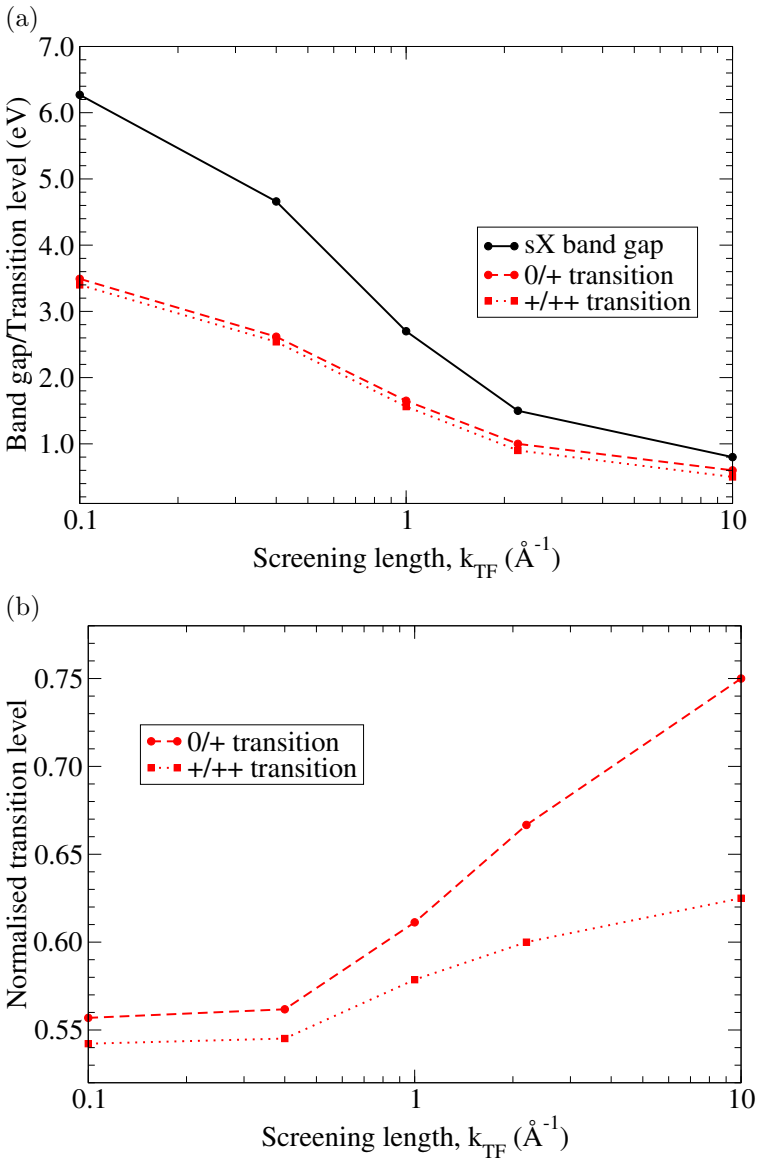

value. The band gap changes slow near the correct value. k_{TF} is proportional to the one sixth power of the valence electron density, so the screening parameter is always in the range of 1.8-2.5Å^{-1}. This slow dependence allows a fixed value of screening parameter to be used if desired, for example in heterogeneous situations such as surfaces or interfaces.

5. Conclusions

To summarise, we analysed the performance of the sX hybrid functional calculation of band structures in this work. The TF screening with average valence electron density is found to give good agreement with experiment. Due to the nature of screening and similar valence density in materials, the screening parameter always falls into a similar range of 1.8-2.5Å^{-1}. This TF screening parameter guarantees that the sX functional are reliable as in the simple systems.

6. Acknowledgements

The authors would like the thank EPSRC for partial funding of this work via the HPC facility Hector under grant EP/K013718/1. This work also made use of the facilities of N8 HPC provided and funded by the N8 consortium and EPSRC grant EP/K000225/1.

References

[1] W Kohn, A D Becke, and R G Parr, *J. Phys. Chem.* **100**, 12974 (1996).
[2] Y Zhao, N E Schultz, and D G Truhlar, *J. Chem. Theory Comput.* **2**, 364 (2006).
[3] M C Payne, M P Teter, D C Allan, T A Arias, and J D Joannopoulos, *Rev. Mod. Phys.* **64**, 1045 (1992).
[4] J P Perdew, K Burke, and M Ernzerhof, *Phys. Rev. Lett.* **77**, 3865 (1996).
[5] A D Becke, *Phys. Rev. A* **38**, 3098 (1988).
[6] L J Sham, M Schluter, *Phys. Rev. Lett.* **51**, 1888 (1983).
[7] J P Perdew and M Levy, *Phys. Rev. Lett.* **51**, 1884 (1983).
[8] M Imada, A Fujimori, and Y Tokura, *Rev. Mod. Phys.* **70**, 1039 (1998).
[9] P Mori-Sanchez, A J Cohen, and W Yang, *Phys. Rev. Lett.* **100**, 146401 (2008).
[10] I A Vladimir, F Aryasetiawan, and A I Lichtenstein, *J. Phys. Condens. Matter.* **9**, 767 (1997).
[11] V I Anisimov, J Zaanen, and O K Andersen, *Phys. Rev. B* **44**, 943 (1991).
[12] N J Mosey and E A Carter, *Phys. Rev. B* **76**, 155123 (2007).
[13] M Hybertsen, S G Louie, *Phys. Rev. B* **34** 5390 (1986).
[14] F Aryasetiawan and O Gunnarsson, *Rep. Prog. Phys.* **61**, 237 (1998).
[15] M von Schilfgaarde, T Kotani, S Faleev, *Phys. Rev. Lett.* **96** 226402 (2006).
[16] M Shishkin, G Kresse, *Phys. Rev. B* **75** 235102 (2007).
[17] J Hong, P Rinke, M Scheffler, *Phys. Rev. B* **86** 125115 (2012).
[18] A Georges, G Kotliar, W Krauth, and M J Rozenberg, *Rev. Modern. Phys.* **68**, 13 (1996).
[19] S Kummel, L Kronik, *Rev. Mod. Phys.* **80**, 3 (2008).
[20] A D Becke, *J. Chem. Phys.* **98**, 5648 (1993).
[21] C Lee, W Yang, R G Parr, *Phys. Rev. B* **37** 785 (1988).
[22] C Adamo and V Barone, *J. Chem. Phys* **110**, 6158 (1999).
[23] J Heyd, G E Scuseria, M Ernzerhof, *J. Chem. Phys.* **118** 8207 (2003).
[24] A V Krukau, O A Vydrov, A F Izmaylov, and G E Scuseria, *J. Chem. Phys* **125**, 224106 (2006).
[25] J E Peralta, J Heyd, G E Scuseria, R L Martin, *Phys. Rev. B* **74**, 073101 (2006).
[26] A Seidl, A Gorling, P Vogl, J A Majewski, and M Levy, *Phys. Rev. B* **53**, 3764 (1996).
[27] B G Johnson, P M W Gill, J A Pople, *J. Chem. Phys.* **98**, 5612 (1993).
[28] J Muscat, A Wander, N M Harrison, *Chem. Phys. Lett.* **342**, 397 (2001).
[29] J Paier, M Marsman, K Hummer, G Kresse, I C Gerber, J G Angyan, *J. Chem. Phys.* **124** 154709 (2006).

[30] W Chen, A Pasquarello, *Phys. Rev. B* **86** 035134 (2012).
[31] F Iori, M Gatti, A Rubio, *Phys. Rev. B* **85** 115129 (2012).
[32] D M Bylander, L Kleinman, *Phys. Rev. B* **41** 7868 (1990)
[33] A J Freeman, *J. Comput. App. Math.* **149** 27 (2002).
[34] S J Clark and J Robertson, *Phys. Rev. B* **82**, 085208 (2010).
[35] K Xiong, J Robertson, M C Gibson, S J Clark, *App. Phys. Lett.* **87**, 183505 (2005).
[36] T Shimazaki, Y Asai, *Chem Phys Lett* **466** 91 (2008).
[37] F Tran, P Blaha, *Phys. Rev. B* **83** 235118 (2011).
[38] M C Gibson, S Brand, and S J Clark, *Phys. Rev. B* **73**, 125120 (2006).
[39] S J Clark, J Robertson, S Lany, and A Zunger, *Phys. Rev. B* **81**, 115311 (2010).
[40] R Gillen, J Robertson, *Phys. Rev. B* **82** 125406 (2010).
[41] Y Guo, S J Clark, and J Robertson, *J. Phys.: Condens. Matter* **24**, 325504 (2012); Y Guo, S J Clark and J Roberton, *J. Chem. Phys.* **140**, 054702 (2014).
[42] R Gillen and J Robertson, *J. Phys.: Condens. Matter* **25**, 165502 (2013).
[43] R Gillen, S J Clark, and J Robertson, *Phys. Rev. B* **87**, 125116 (2013).
[44] M A L Marques, J Vidal, M J T Oliveira, L Reining, S Botti, *Phys. Rev. B* **83** 083119 (2012).
[45] D Koller, P Blaha, F Tran, *J. Phys. Condens. Matter* **25** 435503 (2013).
[46] H K Komsa, P Broqvist, A Pasquarello, *Phys. Rev. B* **81** 205118 (2010)
[47] F Bechstedt, F Fuchs, G Kresse, *Phys Stat Solidi B* **246** 1877 (2009).
[48] J E Moussa, P A Schultz, J R Chelikowsky, *J. Chem. Phys.* **136** 204112 (2012).
[49] V Atalla, M Yoon, F Caruso, P Rinke, M Scheffler, *Phys. Rev. B* **88** 165122 (2013).
[50] M Jain, J R Chelikowsky, and S G Louie, *Phys. Rev. Lett.* **107**, 216806 (2011).
[51] G Cappellini, R Del Sole, L Reining, and F Bechstedt, *Phys. Rev. B* **47**, 9892 (1993).
[52] L H Thomas, *Math. Proc. Cambridge* **23**, 542 (1927).
[53] E Fermi, *Z. Phys. A: Hadrons Nucl.* **48**, 73 (1928).
[54] M D Segall, P J D Lindan, M J Probert, C J Pickard, P J Hasnip, S J Clark, and M C Payne, *J. Phys. Condens. Matter* **14**, 2717 (2002).
[55] H J Monkhorst and J D Pack, *Phys. Rev. B* **13**, 5188 (1976).
[56] J A Stroscio, R M Feenstra, and A P Fein, *Phys. Rev. Lett.* **57**, 2579 (1986).
[57] R I G Uhrberg, G C Hanson, J M Nicholls, S A Flodstrom, *Phys. Rev. Lett.* **48** 860 (1981); P Perfetti, J M Nicholls, B Reihl, *Phys. Rev. B* **36** 6160 (1987); A Cricenti, S Selci, K O Magnusson, B Reihl, *Phys. Rev. B* **41** 12908 (1990).
[58] F Ciccacci, S Selci, G Chiarotti, and P Chiaradia, *Phys. Rev. Lett.* **56**, 2411 (1986).
[59] N J Halas and J Bokor, *Phys. Rev. Lett.* **62**, 1679 (1989).
[60] M Rohlfing and S G Louie, *Phys. Rev. Lett.* **83**, 856 (1999).
[61] J E Northrup, M S Hybertsen, and S G Louie, *Phys. Rev. Lett.* **66**, 500 (1991).
[62] B G Janesko, T M Henderson, G E Scuseria, *Phys. Chem. Chem. Phys.* **11** 443 (2009); T M Henderson, J Paier, G E Scuseria, *Phys. Stat. Solidi B* **248** 767 (2011).
[63] T Cheiwchanchamnangij and W R L Lambrecht, *Phys. Rev. B* **85** (2012).
[64] D Y Qiu, F H daJomada, S G Louie, *Phys. Rev. Lett.* **111** 216805 (2013).
[65] J K Ellis, M J Lucero, G E Scuseria, *App. Phys. Lett.* **99** 261908 (2011).
[66] D Liu, Y Guo, L Fang, J Robertson, *App. Phys. Lett.* **103** 183113 (2013).
[67] G Pacchioni, F Frigoli, D Ricci, *Phys. Rev. B* **63** 054102 (2000).
[68] R Gillen, J Robertson, *Phys. Rev. B* **85** 014117 (2012).
[69] S Lany, A Zunger, *App. Phys. Lett.* **96** 142114 (2010).
[70] J L Lyons, A Janotti, C G van de Walle, *Phys. Rev. Lett.* **108** 156403 (2012).
[71] H-Y Lee, S J Clark, and J Robertson, *Phys. Rev. B* **86**, 075209 (2012).
[72] R Gillen J Robertson, *J. Phys. Condens. Matter* **25** 405501 (2013).
[73] J Lagowski, D G Lin, T P Chen, M Skowronski, H C Gatos, *App. Phys. Lett.* **47** 929 (1985).
[74] E R Weber, H Ennen, U Kaufmann, J Windscheif, J Schneider, T Wosinski, *J. App. Phys.* **53** 6140 (1982).

[75] H K Komsa, A Pasquarello, *Phys. Rev. B* **84** 075207 (2011) .
[76] H K Komsa, A Pasquarello, *J. Phys. Condens. Matter* **24** 045801 (2012).